Exploring a New Candidate of Energy Absorber: Thin-walled Tube Structures Filled with Nanoporous Material Functionalized Liquid

Yueting Sun, Jun Xu, Cang Zhao, Penghui Li, Yibing Li

Abstract Nanoporous material functionalized liquid (NMFL) is now one of the candidates of advanced energy mitigation material, as supported by recent studies. In this study, quasi-static compression experiments and finite element (FE) simulations are conducted to investigate the energy absorption enhancement effect of NMFL as a filler in a thin-walled stainless steel tube. The influence of infiltration pressure (P_{in}), and the interaction effect between NMFL filler and tube wall are comprehensively explored. Results show that the filling with NMFL can enhance the energy absorption capacity of thin-walled tubes under axial compression by 25% at the present configuration, which comes from the nano-scale infiltration of NMFL by converting mechanical energy into excessive interfacial energy, and its interaction effect with thin-walled buckling. P_{in} has a significant impact on the energy absorption characteristics and buckling behavior.

Keywords Energy absorption, nanoporous material, thin-walled tube

I. INTRODUCTION

Developing advanced energy-absorbing materials and structures is recognized as a major solution for the crashworthiness of vehicles. Thin-walled metal tubes and cellular structures are commonly used due to their energy absorption capability during the axial folding [1]. External mechanical energy can be irreversibly converted into plastic strain energy via progressive buckling. The energy absorption capability of thin-walled structures can be further improved by the use of filler. Plenty of studies have been conducted on metal tubes filled by various foams, such as polyurethane foam [2] and aluminum foam [3-4], which verified that foam fillers can improve the deformation behavior and energy absorption capacity of metal tubes. Recently, liquid filled thin-walled and cellular structures attracted more interest [5]. Compared with form fillers, liquid can fit well with various shapes and sizes of structures without mismatch problems, from micro-machines to large industrial equipment. However, conventional liquid is nearly incompressible and this will seriously affect a structure's compressibility.

In our previous work [6-8], the nanoporous materials functionalized liquid (NMFL) proves to have a high energy absorption density, which makes it a viable candidate filler for thin-walled structures. NMFL is a mixture of hydrophobic nanoporous material and liquid. Once external pressure is applied on NMFL, due to capillary effect, liquid cannot enter nanopores until the applied pressure reaches the infiltration pressure P_{in}. During the infiltration process, a large amount of energy can be dissipated by creating interfacial energy at a significantly higher level than traditional materials [9]. As a kind of compressible liquid, NMFL can well accommodate the wall buckling of tube structures, as well as guarantee a high compressibility. Besides, its excellent energy absorption characteristics can be finely tuned according to specific applications. All the above makes it an ideal filler for energy absorbing structures in the automotive industry.

In this study, the energy absorption performance of NMFL-filled stainless steel tube is investigated experimentally and numerically. The quasi-static compression tests are conducted on non-filled tube and NMFL-filled tube. Finite element (FE) simulation is performed to obtain more detailed information. Then, the effect of P_{in} on energy absorption efficiency is investigated, and the interaction effect between NMFL and tube wall is explored. This work may shed light on the application of nanoporous material filled structures in impact

Y. Sun is a PhD student, P. Li is a PhD student, Y. Li is a Prof in State Key Laboratory of Automotive Safety and Energy, Tsinghua University in China (Corresponding author: Yueting Sun, Phone & fax: +86-010-62772721, e-mail: syt06@mails.tsinghua.edu.cn). J. Xu is a PhD student in Earth and Environmental Engineering at Columbia University in USA. C. Zhao is a PhD student of Structural Engineering & Materials Science at University of California, San Diego in USA.

protection, including the passive safety of vehicles.

II. METHODS

Experimental Testing

The experimental set up is depicted in Figure 1(a), composed of a stainless steel (304) thin-walled tube and NMFL inside. Both ends are fixed on stainless steel caps and sealed by J-B Weld epoxy glue. The height is h=6.35 mm, outer diameter is $2R$=6.35 mm and wall thickness is t=0.254 mm. The quasi-static compression tests are conducted on Instron 5582 at 5 mm/min. The energy absorption characteristics can be analyzed based on the force F and displacement δ obtained, with nominal stress $P=F/(\pi R^2)$ and nominal strain $\varepsilon=\delta/h$. For comparison purposes, non-filled tubes are also tested.

NMFL inside the tube is 0.08 g Fluka 100 C_8 reversed phase nanoporous silica gel immersed in deionized water. The average nanopore size is 7.8 nm, specific nanopore volume is 550 mm^3/g. The mechanical characteristics of NMFL can be determined by a quasi-static compression test on NMFL alone [10]. Results are shown in Figure 2 with two cycles of P-ΔV curves, which determines P_{in} to be 16 MPa, that is, water molecules will enter the nanopores on silica gel once the applied pressure on NMFL reaches 16 MPa. When all the nanopores are filled, the infiltration plateau ends and bulk modulus of NMFL increases to that of water, 2.2 GPa. There is no infiltration plateau on the second cycle of P-ΔV curve, suggesting that water infiltrated during the first cycle will not defiltrate out. The mechanical energy is thus absorbed, with a density of 10 J/g for present NMFL.

Computational Modeling

In order to gain more insight into the coupling effect of NMFL infiltration and thin-walled buckling, FE simulation is carried out in ABAQUS. The simulation unit of the NMFL-filled tube is schematically shown in Figure 1(b). The geometry and parent material of the tube is exactly the same as that in the experiment, which is stainless steel 304 with density ρ=8000 kg/m^3, yield stress σ_Y=205 MPa, Young's modulus E = 193 GPa, Poisson's ratio =0.3, the strain hardening exponent 0.45.

The modeling of NMFL is based on its characteristic compression behavior. It exhibits elastic behavior prior to infiltration, and turns into a plastic deformation plateau when applied pressure reaches P_{in}. The last stage is a densification with nanopores filled by liquid. Equation of state (EOS) in ABAQUS/Explicit is applied to simulate NMFL. The linear U_s-U_p Hugoniot form is used to describe the elastic deformation of NMFL, and P-α EOS compaction is adopted to describe its plastic infiltration. NMFL is equivalently treated as a porous material whose solid phase is water, and its plastic crush can well simulate the infiltration process of NMFL. Thus, pressure on the solid phase can be expressed as

$$P_s = f(\rho_s, E_m) = \frac{\rho_0 c_0^2 \eta}{(1-s\eta)^2}(1-\frac{\Gamma_0 \eta}{2}) + \Gamma_0 \rho_0 E_m, \quad (1)$$

where ρ_s is the mass density and E_m is the internal energy density during compression. ρ_0 is reference density, $\eta=1-\rho_0/\rho$. c_0 is sound speed and $\rho_0 c_0^2$ equals the bulk modulus. For water in the present model, ρ_0=1000 kg/m^3, c_0=1497 m/s, slope of U_s-U_p curve s=0, Grüneisen ratio Γ_0=0. Besides, the pressure during the infiltration process can be expressed by P-α EOS compaction as

$$P = \frac{1}{\alpha} f(\rho, E_m), \quad (2)$$

where $\alpha=\rho_s/\rho$. The start pressure P_e and end pressure P_s of the plastic behavior is set according to the infiltration plateau of NMFL.

The tube is fully filled by NMFL and sealed by two rigid panels. The top surface is compressed with a displacement controlled motion and the bottom surface is fixed rigidly. The reaction force and displacement of the top surface is recorded and facilitates the analysis on energy absorption characteristics. An 8-node brick element with reduced integration (C3D8R) is used for NMFL filler. A 4-node shell element with reduced integration (S4R) is used for the sidewall of the tube, with 5 Simpson integration points through the thickness. A convergence study is carried out and an element size of 0.53 mm proves to be sufficient. The interaction between the tube wall and two rigid surfaces are modeled with surface-to-surface contact, and self-contact is used for the tube wall. In this work, the simulation of an NMFL-filled tube and non-filled tube is conducted first, and then the effect of P_{in} is investigated as a parametric study.

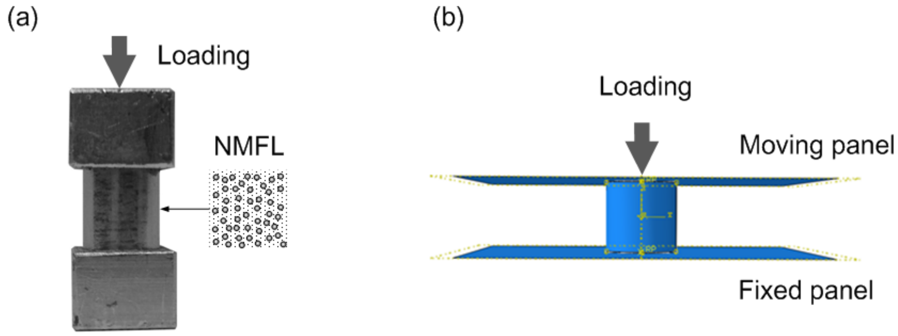

Fig. 1. The experimental setup and simulation unit of NMFL-filled tube
(a) Experimental setup (b) Simulation unit

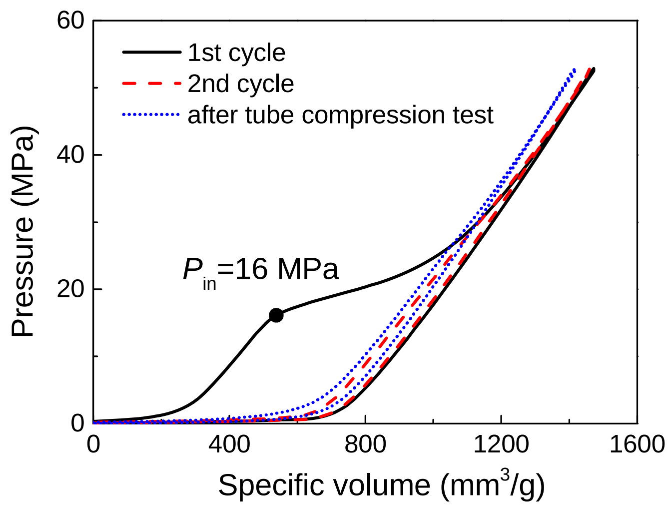

Fig. 2. The *P*-Δ*V* curve of NMFL in compression testing at loading rate of 5 mm/min

III. RESULTS

Testing Results

The experimental stress-strain curves of the non-filled tube and NMFL-filled tube are plotted in Figure 3. The first peak in stress corresponds to the initial collapse when the tube behaves elastically. The major difference lies in the next stage, which shows that the stress plateau of the NMFL-filled tube is much higher than that of the non-filled tube. This is due to the internal support of NMFL during the buckling process. As the NMFL-filled tube is compressed, the inner space of the tube tends to shrink and apply increasing hydrostatic pressure on the liquid inside. Hence the infiltration of NMFL is activated once the pressure inside reaches 16 MPa. During infiltration, NMFL performs as a highly compressible liquid, and thus the buckling of the tube can continue, but with an internal support of 16 MPa. Once the nanopores are filled by liquid, NMFL turns into an incompressible liquid and provides much higher resistance to the further buckling of the tube, which is indicated by an ascent in the stress-strain curve just before ε=0.5. The ending point of infiltration can be finely tuned by the amount and porosity of nanoporous materials. NMFL is collected after the tube compression test to verify that all nanopores have been filled. The *P*-Δ*V* curve obtained is plotted in Figure 2 (dotted line), with no infiltration plateau, indicating that all nanopores have been filled during the tube compression.

As shown in Figure 3, the final crushed shapes (ε=0.5) of the non-filled tube and NMFL-filled tube are similar to each other, since the present P_{in}, 16 MPa is not high enough to globally change the deformation mode of the tube. However, the shape of the NMFL-filled tube is fuller than that of the non-filled tube, indicated by the difference in dent depth of the concave part at the middle. A deeper observation shows that the radius of lobe *r* is significantly smaller for the NMFL-filled tube (r_2<r_1 in Figure 3). The decrease in r is a result of buckling with internal pressure P_{in}. More detailed observation of NMFL's impact on tube buckling will be discussed later. In view of energy absorption, the specific absorbed energy per unit of volume (E) at ε=0.5 of the NMFL-filled tube equals 30 J/cm^3, with a 25% increase compared with 24 J/cm^3 for the non-filled tube. It can be expected that with optimized combination of NMFL and tube parameters, higher energy enhancement can be achieved.

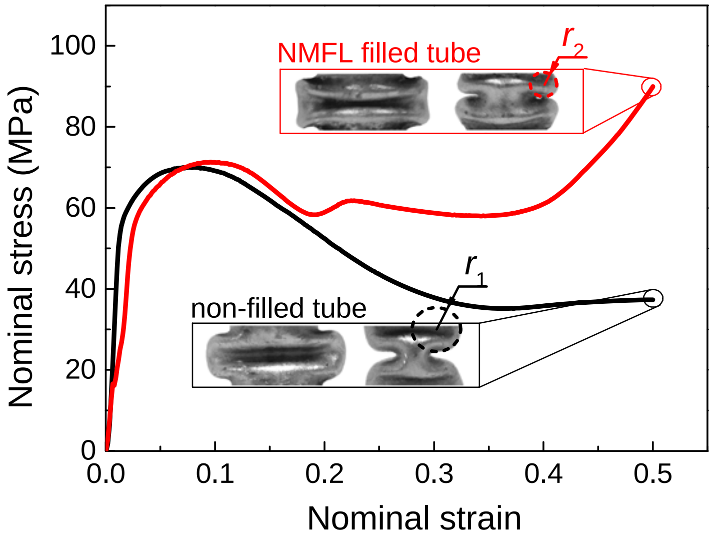

Fig. 3. Experimental compression results of non-filled tube and NMFL filled tube

Simulation Model Verification

Figure 4 shows the numerical stress-strain curves and crushed shapes of the non-filled tube and NMFL-filled tube, which are in good agreement with the experimental results. The pressure of NMFL during the compression is also depicted here to directly reveal the infiltration process of NMFL. The infiltration starts at 16 MPa and ends at 25 MPa just before ε=0.5, which agrees well with the P-ΔV curve of NMFL and the tube compression testing results.

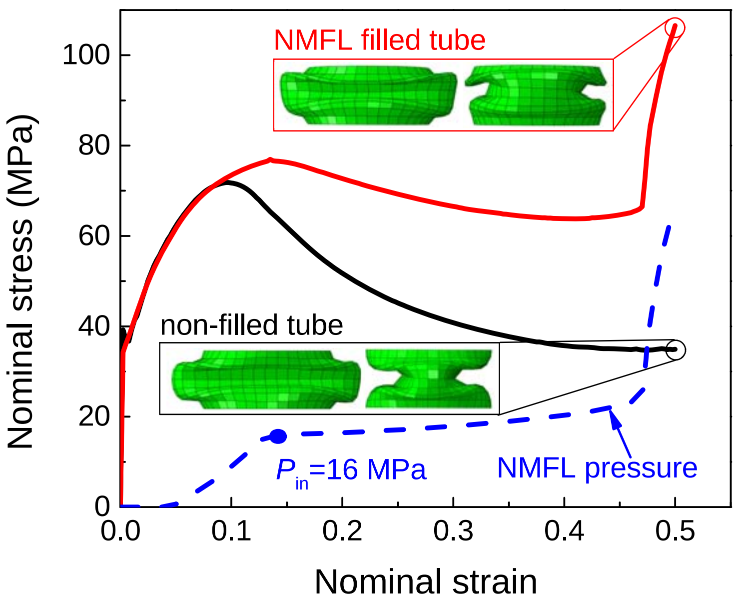

Fig. 4. Numerical compression results of non-filled tube and NNFL-filled tube

Effect of Infiltration Pressure P_{in}

Since P_{in} is a critical factor of the energy absorption characteristic of NMFL, its impact on the compression behavior of the NMFL-filled tube is investigated based on FE simulation. All the geometric and material parameters of tube and NMFL are the same as mentioned above, while P_{in} is selected from 0 MPa (non-filled) to 64 MPa. The porosity of NMFL is set as 0.8, which is sufficiently large for a pure analysis on P_{in}. Little increase in pressure is assigned to the infiltration plateau to simulate nanopores with ideal internal surface. Figure 5 shows the nominal stress-strain curve obtained. As expected, the stress plateau after the first peak increases with P_{in}. Thus, the energy absorbed also increases with P_{in}.

Figure 6 shows the specific absorbed energy E at ε=0.5 with various P_{in}. As P_{in} is increased from 0 MPa to 32 MPa, E increases significantly from 24 J/cm^3 to 37 J/cm^3. However, when P_{in} is further increased above 32 MPa, no more increase in E can be observed. In order to gain more insight, two components of E, the energy absorbed by tube (E_t) and NMFL (E_n), are also plotted in Figure 6. It reveals that E_t increases with P_{in} for the whole range, while E_n increases within 0-32 MPa and decreases within 32-64 MPa. The reason why E_n decreases for higher P_{in} can be explained by Figure 7, which shows the pressure of NMFL (P) during the tube compression. E_n can be simplified as $P \cdot \Delta V$, in which ΔV is the specific volume change of NMFL. Lower P_{in} allows larger ΔV, and higher P_{in} results in limited ΔV. For instance, as P_{in}=8 MPa, infiltration starts at ε=0.1 and lasts for the majority of compression duration, while for high P_{in}=64 MPa, infiltration is not triggered until the end of the compression. Thus, there exists a crest for E_n at certain P_{in}, which is around 32 MPa for the present case. This explains why no more benefit in E can be obtained for further higher P_{in} above 32 MPa. Note that the geometry and material parameters of the tube have prominent impact on E_n, and the crest of E_n varies for different tube cases. Thus, the optimal P_{in} should be determined by taking tube parameters into consideration.

The crush force efficiency (A_E) ratio between average stress and peak stress is also calculated for various P_{in} and shown in Figure 8. As a generally used index for evaluating performance of tube structures, A_E should be as close to 100% as possible in order to absorb maximum energy under a certain stress level. It shows that A_E reaches 0.9 when P_{in} is around 24-32 MPa, compared to 0.67 for the non-filled tube. The improvement in A_E is derived from the enhancement of plateau stress after the peak, so that more energy is absorbed with little increase in peak stress, which is preferable for an energy absorber. However, P_{in} should not be too high since it may cause another peak stress at high strain, and thus lower the crush force efficiency. In such cases, although the amount of energy absorbed is large, the high stress may exceed the damage threshold of the protected object.

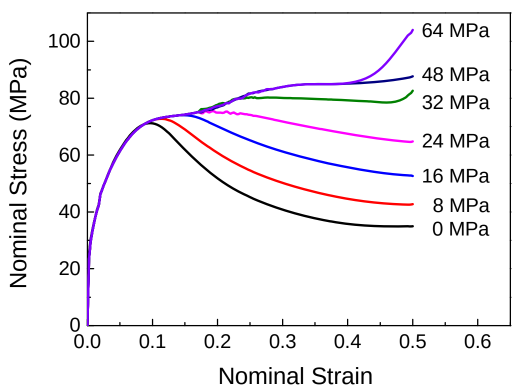

Fig. 5. Nominal stress-strain curves for various P_{in}

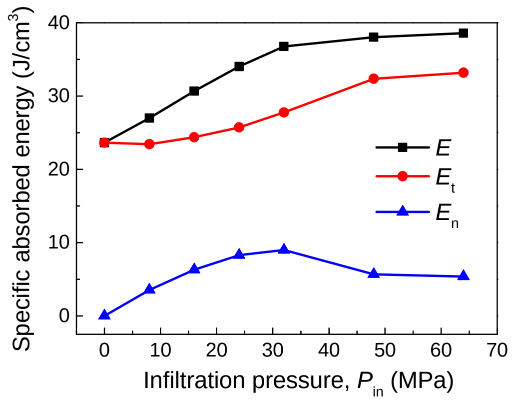

Fig. 6. Specific absorbed energy for various P_{in}

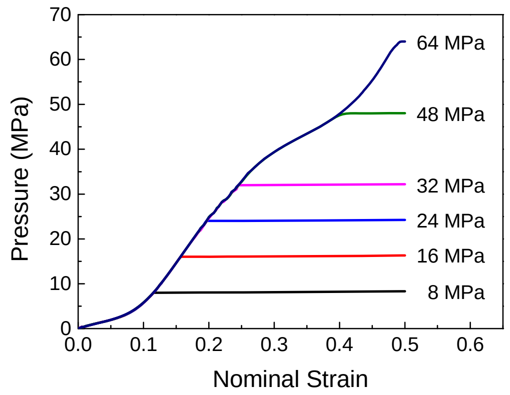

Fig. 7. P (Pressure of NMFL)-strain curve for various P_{in}

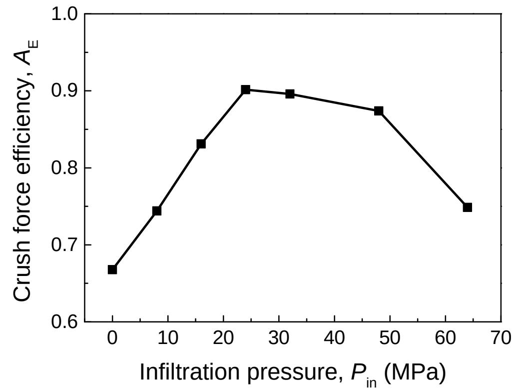

Fig. 8. Crush force efficiency A_E for various P_{in}

Interaction Effect between Tube and NMFL

Figure 9 depicts the nominal stress-strain curve of the non-filled tube, NMFL, NMFL filled tube, and the sum of the non-filled tube and NMFL in one picture for comparison (P_{in}=32 MPa). It shows that stress level of the NMFL-filled tube is higher than the combined effect of the non-filled tube and NMFL, suggesting a certain kind of "interaction effect" between the tube and NMFL during the buckling process. NMFL can affect the deformation mode of the tube wall and thus increase the buckling stress for an additional amount. This may explain the finding in Figure 6 that with NMFL added, the energy absorbed by the tube wall E_t increases. Hence, the final shapes of the tube after compression should be observed to explore the interaction effect.

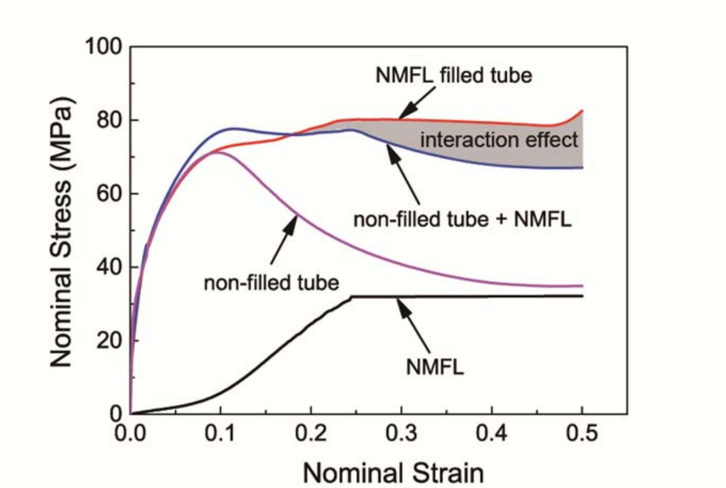

Fig. 9. Schematic of interaction effect

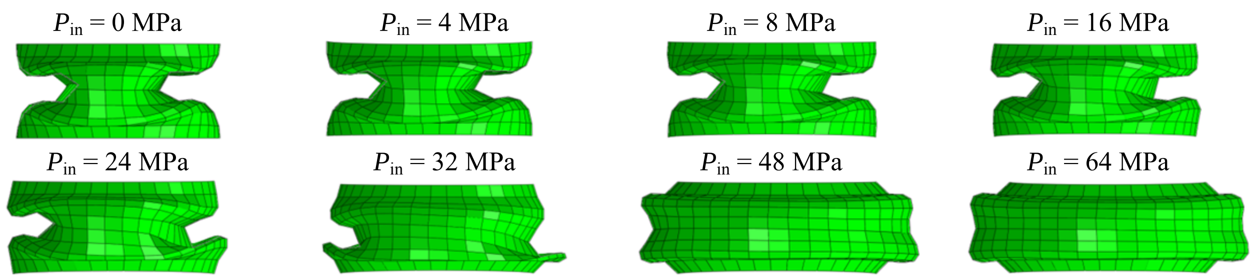

Fig. 10. Vertical sections of NMFL filled tube for various P_{in} at strain=0.5

Figure 10 shows the vertical sections of the NMFL-filled tube with various P_{in} at strain=0.5. Under compression load, the non-filled tube wall (P_{in}=0 MPa) can either deform inward or outward. For the present geometric parameters and boundary conditions at two ends, it is finally shaped into a "dumbbell", with two half lobes at two fixed ends and a concave region at the middle. For the NMFL-filled tube, with liquid serving as a support for tube walls, tube material is hard to move inside, and the effective "resistance" increases with P_{in}. Thus, it can be observed that the dent depth of the concave region decreases with P_{in}.

Further, the radius of lobes decreases with P_{in}. It has been shown in Figure 3 that the radius of lobe *r* will be smaller with NMFL added, and Figure 10 further reveals that *r* decreases with P_{in}. For the case of low P_{in} (such as P_{in}=0 MPa), there are two "half" lobes at two fixed ends. With P_{in} increased (such as P_{in}=32 MPa), the tube material allowed for wrinkle decreases, and thus these "half" lobes transform into small complete lobes gradually. For the case of extremely high P_{in} (such as P_{in}=64 MPa), NMFL keeps elastic for the whole process and strictly prevents any tube wall material to go inside. Consequently, lobes have to be extremely small and finally disappear, and the whole shape is nearly convex and "tire-like".

It has been shown that higher P_{in} can produce a large amount of small lobes, instead of a small amount of large lobes. Hence, higher P_{in} can contribute to a higher buckling stress and higher interaction effect as defined. However, at extremely high P_{in}, the interaction effect will decrease due to less buckling stress needed for the simple convex shape. Figure 11 shows the interaction effect with various P_{in}, indicating that for the present case, interaction effect peaks at P_{in}=32 MPa, which accounts for 19% of the total buckling stress at ε=0.5.

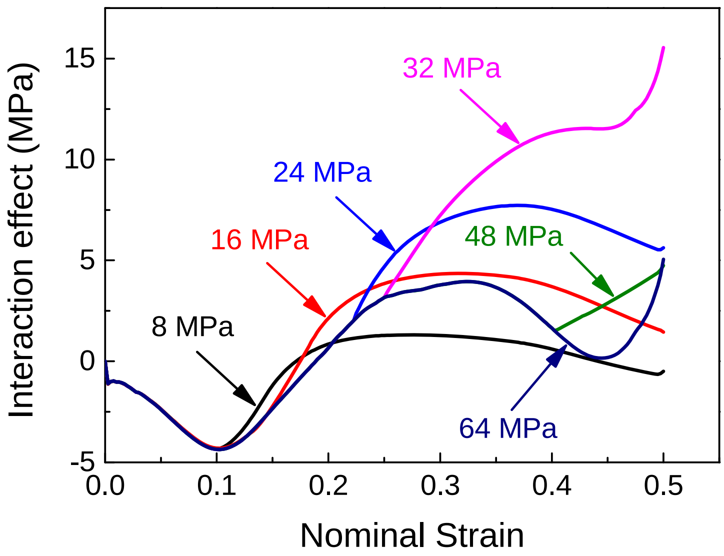

Fig. 11. Interaction effect for various P_{in}

IV. DISCUSSION

It has been validated that the introduction of NMFL can greatly improve the energy absorption of tube structures. With appropriate P_{in}, the energy absorption enhancement can be more than 50% and A_E can reach 0.9. Note that the slenderness ratio of tube in the present work is 1:1 and the energy absorption enhancement of NMFL is not fully utilized due to the limited post-buckling strain. For longer tubes which are generally used in engineering applications, the increased energy absorption capacity can be much higher. Compared with conventional energy absorption materials and structures, an NMFL-filled tube has a higher energy absorption density. For instance, the 37 J/cm^3 (19 J/g) in this study is significantly higher than that of aluminum foam, which is 12 J/cm^3 (12 J/g) at a strain of 0.5 [11-12].

While the present work cannot facilitate the direct application of an NMFL-filled tube, a qualitative direction to design an NMFL-filled tube as a protection device has been presented. As mentioned, the introduction of NMFL has little impact on the peak stress which is determined by the geometry and material parameters of the tube. Thus, a non-filled tube can firstly be selected by setting its peak stress lower than the damage threshold stress of the protected object. Then, the key issue is to maximize A_E by filling the tube with NMFL; that is, raise the plateau stress to the value of peak stress so as to form a square-like stress-strain loading curve. P_{in} should be carefully selected here, normally smaller than the gap between peak stress and plateau stress due to the existence of an interaction effect. Interaction effect is worth considering for a successful design of an NMFL-filled tube, since it may account for up to 20% of the total buckling stress. Actually, an interaction effect can also be observed from tubes filled with solid materials such as aluminium foam [13]. Both solid and liquid filler can act as an elastic-plastic foundation for tube walls and thus reduce the buckling length and produce the interaction effect. However, due to a better match with tube walls, the interaction of NMFL may exhibit certain unique characteristics which are to be explored.

More detailed and quantitative study should be carried out to produce specific formulas to guide the design of NMFL-filled tube structures. Two key parameters of NMFL, P_{in} and porosity, have been involved in this work, which are related to the buckling stress and deformability, respectively. However, tube parameters have not been investigated, including the wall thickness, diameter, yielding stress, etc., which are a part of our future work. With the absence of a quantitative relationship between NMFL and tube parameters, a detailed guide for design of NMFL-filled tube structures cannot be produced. In addition, the present work is limited to a quasi-static situation. As a candidate of impact protection, the dynamic loading behavior of the NMFL-filled tube needs to be investigated. The loading rate effect of NMFL has been examined [14-15], and NMFL proves to have a much higher energy absorption density under impact loading [16]. Hence, it is anticipated that an NMFL-filled tube may have a better performance under impact conditions. Due to the strain rate effect of stainless steel, both the peak stress and plateau stress of non-filled tube will be increased under dynamic condition. Thus, for an optimized design of an NMFL-filled tube, the NMFL should also be rate dependent.

Another problem is the leak of NMFL due to the possible fracture of the tube wall. Note that all the analysis in this work is based on the assumption that no leaking takes place during tube compression, since the leak problem is not noteworthy for the cases in this work up to a strain of 0.5. However, if the infiltration plateau of NMFL is too high or too short, the tube wall may fracture at a certain strain. Thus, appropriate NMFL should be selected to avoid the leak problem. Besides, materials with higher toughness such as polymers can be considered as tube wall material.

V. CONCLUSIONS

The buckling behavior and energy absorption characteristics of NMFL-filled stainless steel tubes are investigated. Through quasi-static compression tests of an NMFL-filled tube and non-filled tube, it is verified that NMFL filler can significantly increase the energy absorption density of tube structures. Based on FE simulation, the effect of P_{in} and interaction between NMFL and tube wall are explored. Results show that the energy absorption enhancement effect of NMFL comes from the infiltration behavior as well as the interaction effect. P_{in} has a prominent impact on the buckling stress and energy absorption characteristics of NMFL-filled tubes. With an optimized P_{in}, NMFL can increase the energy absorption density by more than 50% and A_E can be up to 0.9. Meanwhile, the employment of NMFL will change the buckling mode of the tube wall and thus increase the buckling stress for an additional amount, known as interaction effect. This work may help promote the application of nanoporous materials in energy absorption and protection systems.

VI. ACKNOWLEDGEMENT

The work is supported by International joint research project sponsored by Tsinghua University (20121080050), Individual-research founding State Key Laboratory of Automotive Safety & Energy, Tsinghua University (ZZ2011-112).

VII. REFERENCES

[1] Lu G and Yu TY, *Energy absorption of structures and materials*. 2003: Woodhead Publishing.

[2] Reid S, Reddy T, Gray M. Static and dynamic axial crushing of foam-filled sheet metal tubes. *International Journal of Mechanical Sciences*, 1986, 28(5): 295-322.

[3] Langseth M, Hopperstad O, Hanssen A. Crash behaviour of thin-walled aluminium members. *Thin-Walled Structures*, 1998, 32(1): 127-150.

[4] Hanssen AG, Langseth M, Hopperstad OS. Static and dynamic crushing of square aluminium extrusions with aluminium foam filler. *International Journal of Impact Engineering*, 2000, 24(4): 347-383.

[5] Chen X, Surani FB, Kong X, Punyamurtula VK, Qiao Y. Energy absorption performance of steel tubes enhanced by a nanoporous material functionalized liquid. *Applied physics letters*, 2006, 89(24): 241918.

[6] Sun Y, Xu J, Li Y, Xu X, Liu C, Chen X. Mechanism of water infiltration and defiltration through ZSM-5 zeolite: heating and sodium chloride concentration effect. *Journal of Nanomaterials*, 2013, 2013: 249369.

[7] Sun Y, Xu J, et al. Experimental Study on energy dissipation characteristics of ZSM-5 zeolite/water system. *Advanced Engineering Materials*, 2013, 15(8): 740-746.

[8] Sun Y, Xu J, Li Y, Xu X, Liu C. Effect of pretreatment temperature and sodium chloride concentration on energy dissipation characteristics of ZSM-5/water system. *Journal of Inorganic Materials*, in press.

[9] Xu B X, Qiao Y, Park T, Tak M, Zhou Q L, Chen X. A conceptual thermal actuation system driven by interface tension of nanofluids. *Energy & Environmental Science*, 2011, 4(9): 3632-3639.

[10] Kong X, Qiao Y. Improvement of recoverability of a nanoporous energy absorption system by using chemical admixture. *Applied Physics Letters*, 2005, 86(15): 151919.
[11] Baumeister J, Banhart J, Weber M. Aluminium foams for transport industry. *Materials & design*, 1997, 18(4): 217-220.
[12] Sun Y, Guo Z, Xu J, Xu X, Liu C, Li Y. A candidate of mechanical energy mitigation system: Dynamic and quasi-static behaviors and mechanisms of zeolite β/water system. *Materials & Design*, 2014: in press.
[13] Hanssen A, Langseth M, Hopperstad O. Optimum design for energy absorption of square aluminium columns with aluminium foam filler. *International Journal of Mechanical Sciences*, 2001, 43(1): 153-176.
[14] Chen X, Cao G X, et al. Nanoscale fluid transport: Size and rate effects. *Nano Letters*, 2008, 8(9): 2988-2992.
[15] Han A, Lu W, et al. Effective viscosity of glycerin in a nanoporous silica gel. *Journal of Applied Physics*, 2008, 104(12): 124908.
[16] Surani FB, Kong XG, Panchal DB, Qiao Y. Energy absorption of a nanoporous system subjected to dynamic loadings. *Applied Physics Letters*, 2005, 87(16).